Note: This is a preprint of a paper submitted for publication. Contents of this paper should not be quoted or referred to without permission of the author(s).

To be submitted for publication in *Proceedings of the Spring Meeting of the Materials Research Society*, San Francisco, California, April 27–May 1, 1992

STEP-DRIVEN SURFACE SEGREGATION AND ORDERING DURING Si-Ge MBE GROWTH

CONF-920402--44

DE92 017827

D. E. Jesson and S. J. Pennycook
Solid State Division
Oak Ridge National Laboratory
Oak Ridge, Tennessee 37831-6024

and

J.-M. Baribeau and D. C. Houghton
Institute for Microstructural Sciences
National Research Council of Canada
Ottawa, K1AOR6, Canada

DISCLAIMER

This report was prepared as an account of work sponsored by an agency of the United States Government. Neither the United States Government nor any agency thereof, nor any of their employees, makes any warranty, express or implied, or assumes any legal liability or responsibility for the accuracy, completeness, or usefulness of any information, apparatus, product, or process disclosed, or represents that its use would not infringe privately owned rights. Reference herein to any specific commercial product, process, or service by trade name, trademark, manufacturer, or otherwise does not necessarily constitute or imply its endorsement, recommendation, or favoring by the United States Government or any agency thereof. The views and opinions of authors expressed herein do not necessarily state or reflect those of the United States Government or any agency thereof.

"The submitted manuscript has been authored by a contractor of the U.S. Government under contract No. DE-AC05-84OR21400. Accordingly, the U.S. Government retains a nonexclusive, royalty-free license to publish or reproduce the published form of this contribution, or allow others to do so, for U.S. Government purposes."

SOLID STATE DIVISION
OAK RIDGE NATIONAL LABORATORY
Managed by
MARTIN MARIETTA ENERGY SYSTEMS, INC.
under
Contract No. DE-AC05-84OR21400
with the
U.S. DEPARTMENT OF ENERGY
Oak Ridge, Tennessee

June 1992

MASTER

DISTRIBUTION OF THIS DOCUMENT IS UNLIMITED

STEP-DRIVEN SURFACE SEGREGATION AND ORDERING DURING Si-Ge MBE GROWTH

D. E. JESSON, S. J. PENNYCOOK, J.-M. BARIBEAU,* AND D. C. HOUGHTON*
Solid State Division, Oak Ridge National Laboratory, Oak Ridge, TN, 37831, USA
*Institute for Microstructural Sciences, National Research Council of Canada, Ottawa, K1AOR6, Canada

ABSTRACT

An important role of type S_B step edges in determining the as-grown microstructure of Si-Ge superlattices and alloys is implicated from direct Z-contrast images of as-grown structures. A variety of different ordered phase variants can arise at each Si on Ge interface as a result of vertical segregation during superlattice growth. A new monoclinic-ordered structure is predicted to arise as a result of lateral segregation during alloy growth.

INTRODUCTION

Despite the immense scientific and technological interest in Si-Ge alloys and superlattices [1], little is known about the atomistic mechanisms of growth. Although it is well established that MBE growth occurs via the propagation of surface steps, the atomic-scale processes occurring at step edges remain largely unstudied. In particular, it is not known how such processes influence the atomic-scale structure of alloys and superlattices. The purpose of this paper is to show how we can utilize Z-contrast imaging [2,3] to start to explore the link between atomistic processes at step edges and the atomic-scale structure of alloys and superlattices.

Firstly, we consider some of the atomistic processes likely to occur at step edges. Figure 1 is a schematic representation of Si_xGe_{1-x} alloy growth. The deposited atoms, having given up their heat of condensation, will diffuse across the surface until they reach a step edge. The edge shown in Fig. 1 might represent the edge of a monolayer height island, for example, and atoms will want to attach themselves to the edge giving rise to island growth. However, the sticking probabilities of Si and Ge atoms at the step edge may well be different, and desorption probabilities may also be species specific. It is not difficult to anticipate that such processes might, for example, lead to lateral surface segregation in front of the advancing step edge.

Another interesting possibility is an interchange between a surface adatom and a subsurface atom. Again, such a process is likely to be associated with step edges where the activation barrier for such an interchange would be relatively low. Clearly, this would lead to vertical segregation in the growth direction. We therefore have two distinct possibilities, lateral surface segregation and vertical segregation, both associated with step edges. We now describe how such processes can be accessed experimentally.

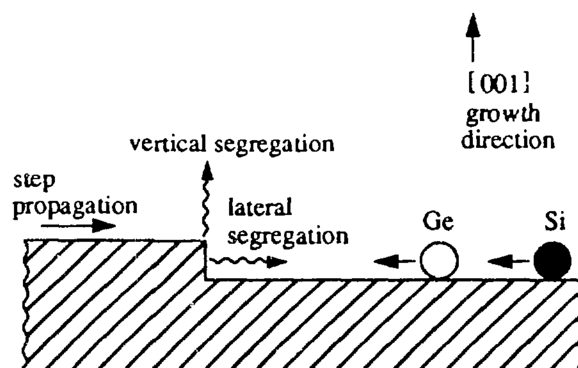

Fig. 1. A schematic representation of Si_xGe_{1-x} alloy growth. The arrows suggest lateral and vertical segregation at the step edge.

At typical MBE growth temperatures (300–600°C), bulk diffusion is negligible, and so the atomistic processes occurring at the surface are essentially frozen in during growth. In this way, the as-grown structure acts as a fossil record of growth and can be accessed by cross-sectional Z-contrast imaging. Lateral segregation can be studied using Si-Ge alloys and vertical segregation processes investigated through imaging Si-Ge superlattices.

VERTICAL SEGREGATION

To illustrate the above ideas, Fig. 2 shows a Z-contrast image of part of an ultrathin $(Si_4Ge_8)_{20}$ superlattice. The image was obtained from the [110] crystal projection which is perpendicular to the direction of step propagation for growth on the (001) surface. Each elongated bright spot in the image corresponds to an atomic dumbbell, and Si and Ge columns are readily distinguished by Z-contrast imaging because of the near atomic number squared sensitivity of high-angle electron scattering [2,3].

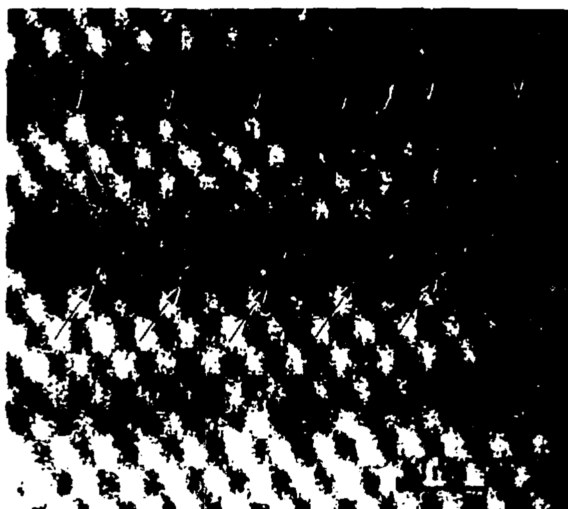

Fig. 2. [110] Z-contrast image of a $(Si_4Ge_8)_{20}$ superlattice which was grown at 350°C at a deposition rate of 0.5 Å s^{-1}.

Of equal importance is the *local* nature of Z-contrast images so that columns can be interpreted completely independently of their neighbors [4]. The bright horizontal bands therefore correspond to deposited Ge layers and the darker bands correspond to deposited Si layers. Remarkably, bright spots can be seen within the Si layers in Fig. 2 which reveals directly that vertical segregation of Ge has occurred into the growing Si layers. What is even more remarkable is that the Ge is ordered. ⟨111⟩ planes of ordered Ge run completely through the central Si layer. In the top Si layer, the ordering is confined to the Si on Ge interface and we observe a (2×n) interfacial periodicity. More elaborate cross-like structures exist in the lower Si layer so that a different ordered phase can exist at each interface. The atomic-scale structure of ultrathin superlattices is therefore far more complicated than previously imagined, and this may well influence the zone folding properties of such structures.

Since the Si on Ge interfaces in Fig. 2 directly represent a fingerprint of the vertical segregation processes, we are in an excellent position to deduce the relevant atomic-scale growth mechanisms. Based on the (2×n) periodicities in our images, we have proposed a novel Ge atom pump mechanism [5–7] which occurs at the rebonded S_B step [8] during monolayer height island growth. This explains everything we see experimentally including the origin of the different ordered phases and the asymmetric interfacial abruptness. We also observe interfacial ordering at isolated Si on Ge interfaces and find that the atom pump operates independently of strain [9].

LATERAL SEGREGATION

We now discuss the topic of Si-Ge alloy growth. Figure 3 shows an image of a $Si_{0.6}Ge_{0.4}$ alloy. The image displays a microtwin and a single long-range ordered phase in the perfect crystal. Clearly, alloy growth at 350°C is very different from the growth of superlattices at the same temperature, where we have observed several phase variants at the Si on Ge interfaces (Fig. 2). The ordering in Fig. 3 consists of alternating Si-rich, Ge-rich ⟨111⟩ planes and the ordering follows a particular ⟨111⟩ direction. This result is actually rather surprising because the sample in Fig. 3 was grown under conditions of very high supersaturation (350°C, 2.4 Å s^{-1} deposition rate), and yet we still observe strong ordering and phase locking.

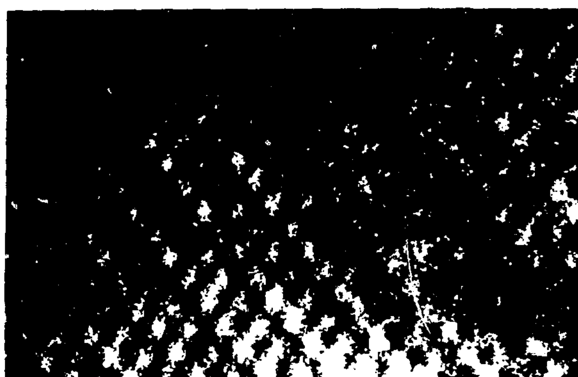

Fig. 3. Z-contrast image of a $Si_{0.6}Ge_{0.4}$ alloy showing a microtwin and long-range ordering.

To explain this behavior, we use the insights gained from the superlattice studies. MBE growth at high supersaturations forces monolayer height islands to grow alternately through high-energy and low-energy S_B steps as shown schematically in Fig. 4. These step edges correspond to the narrow ends of elongated islands observed in STM images [10]. Both steps would prefer Ge atoms to occupy the shaded binding sites, since Ge has the lowest energy level in the wells. However, in the case of alloy growth, there is no longer any need to pump subsurface Ge at the step edge since Ge atoms are readily available on the surface in the two dimensional reservoir of atoms surrounding the growing island. Hence, we have a lateral segregation problem.

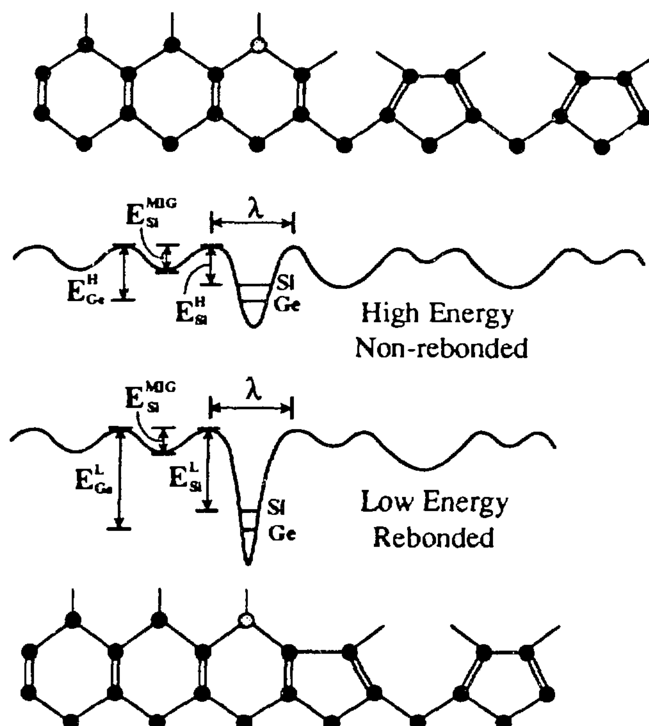

Fig. 4. [110] projection of high-energy nonrebonded and low-energy rebonded type-S_B steps with accompanying energy-level schematics (see text).

A rate equation analysis of island growth [11] enables the Si concentration at the low- and high-energy S_B steps to be calculated as a function of growth temperature (Fig. 5). At low temperatures, both binding sites have the same composition since the steps act as perfect atom traps, freezing the incoming flux at the composition of the deposited alloy. At high temperatures, the model also predicts no ordering. Physically, this is due to the frequent arrival and desorption rate of atoms at the step edges. Both steps will compete for Ge and tend towards equilibrium segregation with the reservoir. It is this competition that leads to the absence of ordering at high temperatures. An ordering peak is, however, present at intermediate temperatures where the two steps behave very differently as a result of nonequilibrium growth. The low-energy step acts as an effective atom trap, whereas the high-energy step approaches its Ge-rich equilibrium segregation value. Si rejected by this high-energy step will be quenched at the low-energy step, so that growth-induced compositional ordering results [11].

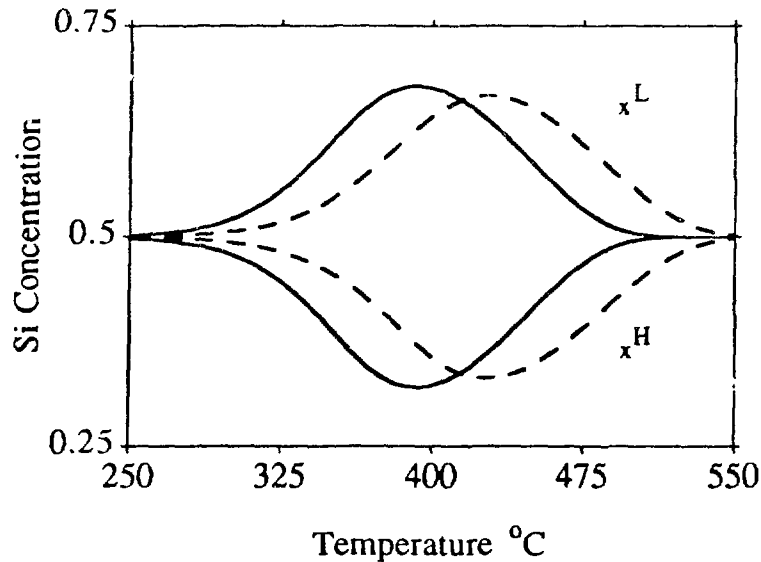

Fig. 5. Si concentration at low-energy (upper curves) and high-energy (lower curves) S_B steps as a function of substrate temperature for a $Si_{0.5}Ge_{0.5}$ deposited alloy. The solid and dashed lines correspond to deposition rates of 0.24 and 0.8 nms^{-1}, respectively.

Since the energy levels at step edges are not accurately known, the uniqueness of the results presented in Fig. 5 deserves some consideration. It turns out that the most important factor influencing the peak position is the absolute well depth which is set by the Si desorption energy E^L_{Si}. Assuming E^L_{Si} = 1.47 eV, we can explain the experimentally observed temperature dependence of the ordering [11]. The position of the relative energy levels mainly affects the ordering parameter. Thus, the calculation of Fig. 5 demonstrates that step energies are in the correct range to explain ordering entirely as a surface effect consistent with nonequilibrium growth. Given this fact, we can now predict the effect of increasing the deposition rate as shown by the dashed line of Fig. 5. The ordering peak has clearly shifted out to a higher temperature. This is physically reasonable since we are making the steps grow faster and are consequently extending the kinetic trapping regime. Thus, ordering is sensitive to both temperature and deposition rate, and this overall dependence on the degree of supersaturation might explain why it has been notoriously difficult to reproduce ordering results between different growth groups [12–15].

The lateral segregation model naturally explains the origin of the ordering, although we have still to explain the phase locking behavior. As discussed in Ref. [11], we anticipate that the strain set up by the ordered monolayer starts to influence the direction of dimerization during the initial stages of island nucleation. The system then naturally phase locks into one of the four possible orientational variants (although translational variants are also possible). It is likely, as in the case of GaAs on Si growth [16], that antiphase boundaries are eliminated with increasing film thickness so that there is a depth evolution of the domain structure.

Another important point inherent in our lateral segregation model is that the ordering is independent of the direction of step propagation. This explains why many phase variants arise in the case of superlattice growth but only a single phase exists in the case of alloy growth. However, a big surprise from our ordering model is that the phase predicted is different from the two rhombohedral structures RS1 and RS2 which have been previously proposed by Ourmazd and Bean [15] to explain ordering in alloys. Instead, we predict the new monoclinic structure MS1 (space group Bm) as shown in Fig. 6. This structure is simultaneously ordered along two sets of ⟨111⟩ planes and is consistent with all previous diffraction data [15,17] although it has not been considered to explain ordering in alloys. Image simulation of the ordered phase provides excellent agreement with experiment. Our lateral surface segregation model, in which ordering is the result of highly nonequilibrium growth at large supersaturations, is therefore entirely consistent with the anticipated monolayer height island growth conditions [18]. This should be viewed as an alternative explanation to the surface stress-induced alloy ordering model proposed by LeGoues et al. [19], which requires bilayer step-flow conditions together with appreciable subsurface interdiffusion. In fact, under conditions of bilayer step flow, our lateral segregation model also predicts that the RS2 structure will occur but avoids the need for substantial subsurface diffusion. Thus, ordering may provide a new way of studying growth kinetics during alloy growth [20].

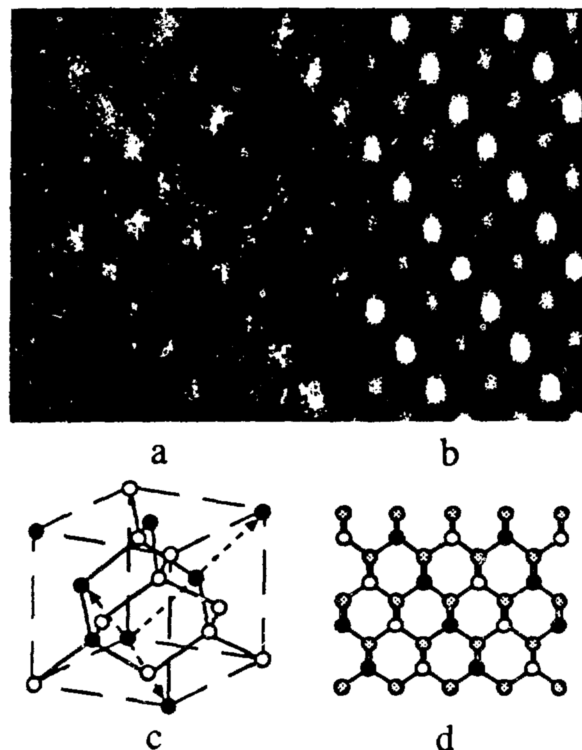

Fig. 6. (a) [110] Z-contrast image of an ordered $Si_{0.6}Ge_{0.4}$ alloy deposited at 0.24 nms^{-1} on a Si(001) substrate at 350 ± 25°C. The accompanying simulation (b) is generated from the [110] projection (d) of the ordered phase (c) predicted by our lateral segregation model. Each bright spot in the image corresponds to a [110] dumbbell, and the column intensities approach the atomic-number-squared dependence of unscreened Rutherford scattering. The open, solid, and shaded circles represent Ge-rich, Si-rich, and deposited alloy compositions, respectively. In (c) the dashed arrows define a primitive unit cell of the ordered phase.

CONCLUSIONS

In conclusion, we have presented a new view of growth-induced ordering during Si-Ge MBE growth. Atomic rearrangements at step edges can explain the ordered structures observed in Si-Ge superlattices and alloys, and indeed similar considerations might be applied to explain ordering in III-V materials. Our cross-sectional imaging of "surface processes" should be applicable to a wide variety of epitaxial growth problems including atomic mechanisms of surfactants and dopant incorporation. Our experience with the Si-Ge system suggests we are only beginning to unravel the immense complexities of semiconductor growth on the atomic scale.

ACKNOWLEDGEMENT

We would like to thank S. L. Carney, T. C. Estes, and J. T. Luck for technical assistance. This research was sponsored by the Division of Materials Sciences, U.S. Department of Energy, under contract DE-AC05-84OR21400 with Martin Marietta Energy Systems, Inc.

REFERENCES

1. See, for example, *Silicon Molecular Beam Epitaxy*, edited by J. C. Bean, S. S. Iyer, and K. L. Wang, *Mat. Res. Soc. Proc.* **220** (1991).

2. S. J. Pennycook and D. E. Jesson, *Phys. Rev. Lett.* **64**, 938 (1990).

3. S. J. Pennycook and D. E. Jesson, *Ultramicroscopy* **37**, 14 (1991).

4. D. E. Jesson, S. J. Pennycook, and J.-M. Baribeau, p. 938 in *High Resolution Electron Microscopy of Defects in Materials*, edited by R. Sinclair, D. J. Smith, and U. Dahmen, *Mat. Res. Soc. Proc.* **183**, Pittsburgh, Pennsylvania, 1990.

5. D. E. Jesson, S. J. Pennycook, and J.-M. Baribeau, *Phys. Rev. Lett.* **66**, 750 (1991).

6. D. E. Jesson and S. J. Pennycook, *MRS Bulletin* **16**, No. 3, 34 (1991).

7. D. E. Jesson and S. J. Pennycook, *Scanning* **13**, Suppl. I, 65 (1991).

8. D. J. Chadi, *Phys. Rev. Lett.* **59**, 1691 (1987).

9. D. E. Jesson, S. J. Pennycook, and J.-M. Baribeau, p. 141 in *Silicon Molecular Beam Epitaxy*, edited by J. C. Bean, S. S. Iyer, and K. L. Wang, *Mat. Res. Soc. Proc.* **220** (1991).

10. R. J. Hamers, U. K. Köhler, and J. E. Demuth, *J. Vac. Sci. Technol.* **A8**, 195 (1990).

11. D. E. Jesson, S. J. Pennycook, J.-M. Baribeau, and D. C. Houghton, *Phys. Rev. Lett.* **68**, 2062 (1992).

12. D. J. Lockwood, K. Rajan, E. W. Fenton, J.-M. Baribeau, and M. W. Denhoff, *Solid State Commun.* **61**, 465 (1987).

13. T. S. Kuan, S. S. Iyer, and E. M. Yeo, p. 580 in *Proc. of Forty-Seventh Annual Meeting EMSA*, San Francisco Press, San Francisco, 1989.

14. F. K. LeGoues, V. P. Kesan, T. S. Kuan, and S. S. Iyer, p. 100 in *Proc. of the First Topical Symposium on Si Based Heterostructures,* Toronto, 1990 (unpublished).

15. A. Ourmazd and J. C. Bean, *Phys. Rev. Lett.* **55**, 765 (1985).

16. S. Iyer, H. Morkoc, H. Zabel, and N. Otsuka, Comments on *Cond. Mat. Phys.* **15**, 1 (1989).

17. F. K. LeGoues, V. P. Kesan, and S. S. Iyer, *Phys. Rev. Lett.* **64**, 40 (1990).

18. A. J. Hoeven, E. J. Van Loenen, D. Dijkkamp, J. M. Lenssinck, and J. Dieleman, *Thin Solid Films* **183**, 263 (1989).

19. F. K. LeGoues, V. P. Kesan, S. S. Iyer, J. Tersoff, and R. Tromp, *Phys. Rev. Lett.* **64**, 2038 (1990).

20. D. E. Jesson, J. Z. Tischler, S. J. Pennycook, J.-M. Baribeau, and D. C. Houghton (to be published).